

# Catalysis Science & Technology

Accepted Manuscript

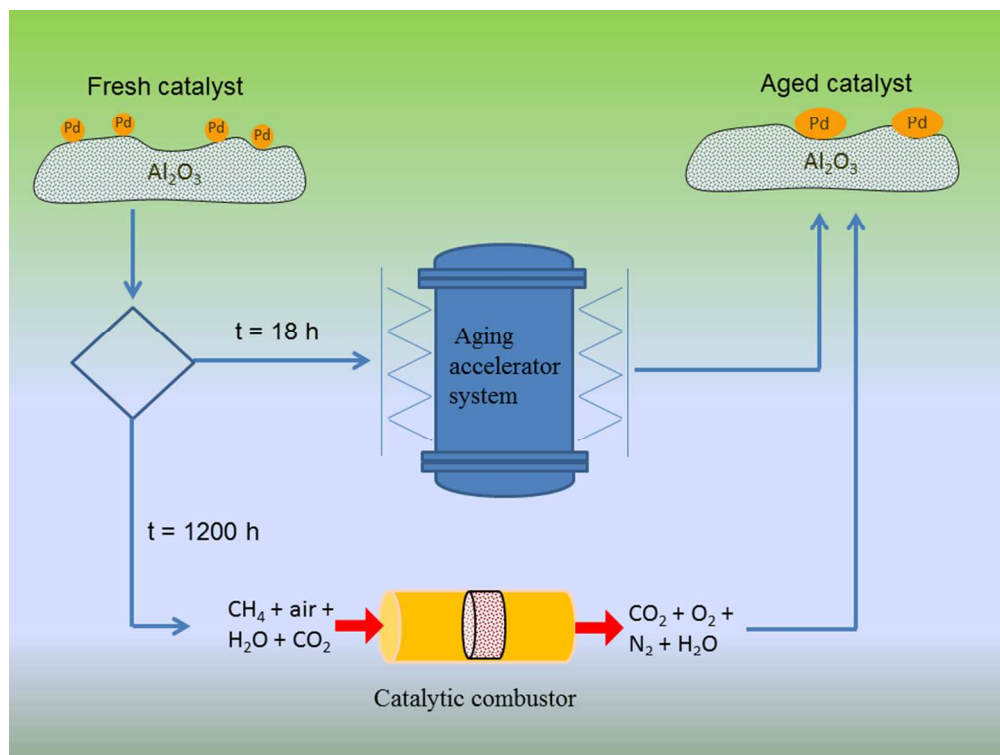


This is an *Accepted Manuscript*, which has been through the Royal Society of Chemistry peer review process and has been accepted for publication.

*Accepted Manuscripts* are published online shortly after acceptance, before technical editing, formatting and proof reading. Using this free service, authors can make their results available to the community, in citable form, before we publish the edited article. We will replace this *Accepted Manuscript* with the edited and formatted *Advance Article* as soon as it is available.

You can find more information about *Accepted Manuscripts* in the [Information for Authors](#).

Please note that technical editing may introduce minor changes to the text and/or graphics, which may alter content. The journal's standard [Terms & Conditions](#) and the [Ethical guidelines](#) still apply. In no event shall the Royal Society of Chemistry be held responsible for any errors or omissions in this *Accepted Manuscript* or any consequences arising from the use of any information it contains.



254x190mm (96 x 96 DPI)

## Accelerated hydrothermal ageing of Pd/Al<sub>2</sub>O<sub>3</sub> for catalytic combustion of ventilation air methane

Cite this: DOI: 10.1039/x0xx00000x

Adi Setiawan,<sup>a,b</sup> Jarrod Friggieri,<sup>a</sup> Glenn Bryant,<sup>a</sup> Eric M. Kennedy,<sup>a</sup> Bogdan Z. Dlugogorski,<sup>c</sup> and Michael Stockenhuber <sup>\*a</sup>

Received 00th January 2012,  
Accepted 00th January 2012

DOI: 10.1039/x0xx00000x

[www.rsc.org/](http://www.rsc.org/)

In this report, the characteristics of Pd/Al<sub>2</sub>O<sub>3</sub> catalyst after long-term stability tests in catalytic combustion of simulated ventilation air methane gas were investigated with the objective of understanding catalyst deactivation phenomena. It was found that the deactivation is primarily due to palladium migration and particle growth and is the most prominent in the presence of water vapour. The formation of  $\alpha$ -Al<sub>2</sub>O<sub>3</sub> during long-term stability tests explains the changes in pore structures which is responsible for re-dispersion of palladium particles. Four accelerated ageing procedures were performed with an aim of mimicking the properties of used catalysts which have been operating continuously for extended time periods (over 1100 h). XRD patterns of aged catalysts disclose the absence of an alpha-alumina phase, suggesting that the transformation of alumina phase occurred at a very slow rate. Among the four procedures, ageing under wet-oxidizing atmosphere provides the catalyst bed that is the best matches to the properties of long-term used catalysts in terms of performance and the characterization employed. Increasing the aging temperature up to 830 °C leads to depletion of surface palladium, which permanently reduces the performance of the catalyst.

### A Introduction

Methane is a gas with significant greenhouse warming potential whose atmospheric sources and sinks are well documented.<sup>1</sup> Nearly 10 % of total anthropogenic methane emissions originate from coal mining activities,<sup>2</sup> and almost two-thirds of these emissions originate from mine ventilation air. Reducing the greenhouse impact of this particular source presents significant challenges to mine operators, the most notable being that ventilation air methane (VAM) is a low concentration, high volume stream that prevents the use of conventional combustion and energy recovery technologies. Low temperature catalytic combustion offers an alternative treatment method, which, when compared to high temperature combustion, offers the advantage to eliminate the generation of additional emissions to the air, such as nitrogen oxides. However, its viability depends on maintaining the activity of the catalyst bed during its exposure to high volumes of ventilation air that contains several components which have the potential to affect performance, such as water vapour and particulate matter.

It is widely accepted that supported palladium catalysts are one of the most effective in the low temperature oxidation of methane.<sup>3</sup> Under oxygen-rich conditions, PdO is formed and represents the active phase for methane oxidation.<sup>3</sup> It is suggested that water produced by reaction inhibits the activity of Pd-based catalysts due to competition with methane for the active sites.<sup>4-6</sup> Furthermore, the presence of water in the feed induces a transformation of the active sites (oxidised Pd) into a less active sites (most likely hydroxy species) and results in permanent deactivation.<sup>4-7</sup> The rate of catalyst deactivation due to water, either present in the feed or produced in the reaction, has a strong dependency from reaction temperature.<sup>4, 7</sup> Our recent evaluation of Pd/Al<sub>2</sub>O<sub>3</sub> catalysts over long-term time-on-stream (TOS) experiments suggests that the deactivation process is a complex phenomenon, although, as highlighted in other studies, the presence of water in the feed stream is perhaps the most significant factor contributing to catalyst deactivation.<sup>8</sup>

Despite considerable effort, the mechanism of catalyst deactivation is not fully understood.<sup>9</sup> Deactivation can occur through chemical, mechanical and thermal processes.<sup>10</sup> Thermal

deactivation processes include the loss of active-site surface area as a result of particle aggregation and collapse of the support pore structure through re-crystallization. Chemical transformation can also result in the loss of active metal sites.<sup>10</sup>

These deactivation processes can be accelerated under high-temperature hydrothermal ageing. A study of hydrothermal ageing on methane combustion over Ce-promoted PdO/ZrO<sub>2</sub> catalysts highlighted the impact that ageing temperature plays on catalyst deactivation.<sup>11</sup> Hydro-thermal treatments for two weeks on various supported Pd catalysts at 900 °C under simulated domestic boiler exhaust gas were performed to understand the ageing mechanism in natural gas combustion.<sup>12</sup> Deactivation studies were reported recently for natural-gas vehicle catalysts<sup>13</sup> and diesel oxidation catalysts<sup>14</sup> where significant changes in morphology and chemical poisoning were observed. A very recent article reported that support phase transformation and particle sintering were found after thermal (at 900 °C in air) and stoichiometric (at 900 °C, air-fuel equivalent ratio = 1) ageing over Pd/YFeO<sub>3</sub> three-way-catalyst.<sup>15</sup> However, the effects caused by thermal ageing and chemical poisoning are still inconclusive, and, in particular, the ageing process under simulated VAM gas has not been considered.

In this contribution, we report the properties of Pd/Al<sub>2</sub>O<sub>3</sub> catalyst after long-term stability tests in the presence of water and coal mine dust in lean-methane combustion. Catalyst deactivation has also been explored using four accelerated ageing procedures. Catalysts were aged under a wet feed at 780 °C and 830 °C for 18 h (the wet feed containing CH<sub>4</sub>, H<sub>2</sub>O and air), under a wet-oxidizing mixture at 780 °C for 18 h, and in an autoclave at 175 °C for 3 days. The properties of the aged catalysts were compared with the properties of used catalysts tested in long-term stability experiments. Our overarching aim is to gain a better understanding of the deactivation phenomena and to explore effective strategies for accelerating the ageing process in order to reduce the time that is typically required for catalyst stability tests.

## B Experimental

### Catalyst treatment

The material used in the study (1.0 wt% Pd/Al<sub>2</sub>O<sub>3</sub>) was supplied by Sigma-Aldrich. Following our previously reported procedure,<sup>8</sup> prior to use, the material was activated by calcining in air at 500 °C for 2 h then reduced by purging in H<sub>2</sub> for 2 h at 300 °C. We subsequently denote this sample as “calcined-reduced” while the “fresh” catalyst is referred to “as received catalyst”.

We begin by characterising samples used in ventilation air methane (VAM) treatments reported earlier.<sup>8</sup> Three samples were selected from the long-term studies, which will be referred to as “dry-VAM”, “wet-VAM” and “wet-dust-VAM”. The dry-VAM sample was tested for 1600 h time on stream (TOS) in a feed consisting of 0.7 % CH<sub>4</sub> balanced with air. The wet-VAM sample was subjected to a feed of 0.7 % CH<sub>4</sub>, 1 % CO<sub>2</sub>, 3 % – 4 % H<sub>2</sub>O balanced with air for 1150 h TOS. A similar feed was used for the wet-dust-VAM sample, with the addition of VAM dust being packed in front of the catalyst bed. The experimental procedures of these long-term experiments were detailed in our previous report.<sup>8</sup>

In an effort to identify an accelerated ageing protocol that emulates the deactivation processes occurring in the long-term experiments, four aging treatments were examined. The possibility of increasing bed temperatures caused by coal-dust channelling/combustion observed in our previous work also motivates our assessment of the catalyst performance at higher temperatures. Treatment I involved aging at a bed temperature of 780 °C for 18 h under a feed of 0.7 % CH<sub>4</sub>, 3 vol% H<sub>2</sub>O balance air. Treatment II used the same feed as I, but was aged at 830 °C for 18 h. Treatment III involved aging at 780 °C for 18 h under a mixture of 60 vol% O<sub>2</sub>, 3 vol% H<sub>2</sub>O and the balance being helium. Aging under a wet oxygen bath gas was chosen to promote the formation of palladium oxide, which was observed to be the only Pd species present after the long-term studies.<sup>8</sup> Treatment IV employed hydrothermal aging in an autoclave set at 175 °C for three days to promote the deactivation of the catalyst by water. After the ageing treatments, the catalytic activity of each sample was tested for methane oxidation under humid conditions (feed consisted of 0.7 % CH<sub>4</sub>, 3.2 % H<sub>2</sub>O, balance air) at a gas hourly space velocity (GHSV) of 100000 h<sup>-1</sup>.

### Catalyst Characterization

The surface area, pore size and pore volume of the catalyst samples were measured by nitrogen adsorption-desorption at 77 K using a Micromeritics TriStar 3000 physisorption analyzer. Palladium loading was quantified using a Varian 715-ES inductively coupled plasma optical emission spectrometer (ICP-OES). Zeiss Sigma VP FESEM served to capture the Scanning Electron Microscopy (SEM) images of the sample using a secondary electron (SE) detector and backscattered electron (BE) detector. Bruker light element SSD Energy-dispersive X-ray spectroscopy (EDS) detector allowed the elemental analysis while capturing the SEM images. A JEOL 2200 FS transmission electronic microscope (TEM) featured with EDS and scanning transmission electron microscope (STEM) system was used for imaging nano-sized Pd particles and support as well as measuring the particle size distribution. TEM particle analysis was carried out using Gatan DigitalMicrograph software. Powder X-Ray diffraction patterns of fresh and used catalysts were collected using Cu K $\alpha$  radiation with a Philips X'Pert diffractometer. Diffractograms were recorded in the 2 $\theta$  angle range from 2° to 90° with 0.008° 2 $\theta$  step resolution.

For surface analysis, ex-situ X-ray photoelectron spectroscopy (XPS) was carried out using mono-chromated Al K alpha (energy 1486.68 eV) radiation and the emitted photoelectrons were analyzed using an ESCALAB250Xi manufactured by Thermo Scientific, UK. To avoid sample contamination, the used samples were immediately transferred into sealed container after terminating the reaction by cooling in helium. The exposure time of samples in air was minimized to reduce the likelihood of experimental artefacts especially those related to adsorption of water vapour from ambient air. The sample was mounted on the sample holder using indium foil. The energy scale was shifted relative to the adventitious carbon at 284.6 eV. The shift was cross checked with the position of O 1s from Al<sub>2</sub>O<sub>3</sub> which is found at 531 eV. Fitting of component contributions to the peaks was performed using a mixed Gaussian-Lorentzian (30:70) line-shape.

### Catalytic activity measurement

The activity of the catalyst was measured in a tubular stainless steel micro reactor. For accelerated ageing experiments, the feed was 7000 ppm CH<sub>4</sub>, 30000 ppm H<sub>2</sub>O balanced with air at a GHSV of 100000 h<sup>-1</sup>. The inlet and outlet mixtures were analyzed using a gas chromatograph equipped with a thermal conductivity detector (TCD) and concentric packed column (Alltech CTR-I). Water was added as a reactant by passing the feed through a saturator and a humidity probe (Pico HumidProbe AT329/21) was installed at the outlet. The actual reaction temperature was observed by placing a thermocouple close to the catalyst bed. For the long-term catalytic stability tests, a separate set-up was prepared and running continuously under wet condition as reported in our earlier work.<sup>8</sup>

## C Results and discussion

### The nature of fresh and used Pd/Al<sub>2</sub>O<sub>3</sub> catalysts

In the long-term time-on-stream (TOS) studies catalyst deactivation was monitored as an increase in bed temperature required in order to maintain methane conversion at 90 %. Fig. 1 plots the variation of temperatures at 90 % conversion ( $T_{90}$ ) versus time-on-stream for the three VAM sample conditions. In all cases, a significant level of catalyst deactivation occurs in the first 50 h TOS. This is followed by a much more gradual decay in bed activity, and after a few hundred hours the bed activity stabilises at a relatively constant value. At the end of the experiments the catalyst beds reached 450 °C (1600 h) in the case of dry-VAM, and 500 °C for wet-VAM (1110 h). The reduction in catalyst activity resulting from the presence of water in the feed is readily apparent in these data. The wet-dust

VAM experiment displayed some instability in the bed temperature set point, which was attributed to coal particle combustion and channelling during the run,<sup>8</sup> after repacking the bed, the final bed temperature was similar to that of wet-VAM experiment. The used catalysts were transferred carefully into sealed containers and subsequently characterized using XPS, N<sub>2</sub>-physisorption, XRD, SEM and TEM analyses. The XPS analysis results are reported in<sup>8</sup>.

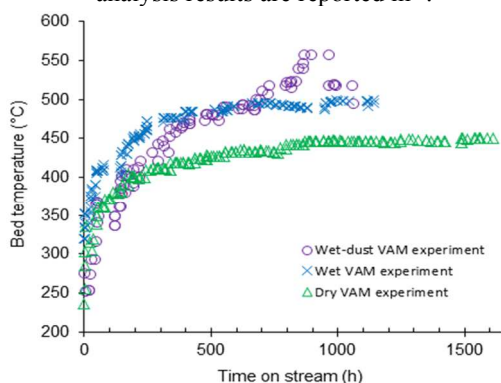


Fig. 1. Catalyst bed temperature required for 90 % CH<sub>4</sub> conversion over 1.0 Pd/Al<sub>2</sub>O<sub>3</sub> catalyst. Feed = 0.7 % CH<sub>4</sub>, 1 % CO<sub>2</sub>, 3–4 % H<sub>2</sub>O (for wet feeds) balance air. GHSV = 100000 h<sup>-1</sup>.  $\Delta$  = dry VAM experiment;  $\times$  = wet VAM experiment and  $\circ$  = wet-dust VAM experiment.

The nitrogen adsorption-desorption isotherms of all tested samples are of type IV as classified by International Union of Pure and Applied Chemistry (IUPAC),<sup>16</sup> suggesting the materials are meso-porous, and that only minor changes in pore structure originate from the long-term stability tests. The surface area of the samples was calculated using the Langmuir method, and the results are provided in Table 1. These data suggest that the pore structure of the supports changed at a very slow rate.

XRD patterns of the samples are plotted in Fig. 2, and are dominated by reflections by  $\gamma$ - and  $\theta$ -alumina phases. Reflections by Pd or PdO are expected to be very weak and overlapped by the alumina peaks, but can be distinguished as slightly increased intensities and widths of the support reflections. These are very difficult to distinguish in the fresh or calcined-reduced sample, but peaks assigned to PdO can be seen in the used catalyst patterns (Fig. 2b-2d),<sup>17, 18</sup> suggesting agglomeration of Pd particle during the runs. In addition, peaks assigned to  $\alpha$ -alumina can be seen in the dry-VAM and wet-VAM patterns.

At temperatures > 900 °C,  $\gamma$ -alumina is gradually transformed to  $\delta$ -alumina, and to  $\alpha$ -alumina via  $\theta$ -alumina at temperatures > 1100 °C.<sup>19</sup> These transformations result in a dramatic decrease in surface area. It is surprising that we observe such transformations of the support temperatures as low as 450 °C, admittedly over long periods of time, in the case of both dry- and wet-VAM samples. Whilst these two samples also display the most notable decrease in surface area (Table 1), the fact that the transition does not occur in the sample with dust makes it difficult to attribute the loss in activity to this particular support phase transformation. This may reflect the fact that the reaction atmosphere plays a significant role in promoting structural changes and crystallisation of the support.<sup>20</sup>

Fig. 3 shows the SEM images of calcined-reduced and used catalysts. No palladium particles are visible in the image of the calcined-reduced catalyst (Fig. 3a), most likely due to the low Pd loading and very small particle size. In contrast, after 1600 h TOS under dry-VAM gas, the SEM image (Fig. 3b) reveals very small bright dots (see the arrow) spread over the surface of the support. Using EDS analysis, the bright dot on this image was identified as a palladium particle. Similar particles were observed also from used catalysts of wet-VAM and wet-dust-VAM experiments (Fig. 3c-3d), suggesting re-dispersion or particle agglomeration occurred during these long-term experiments. The SEM images therefore support the XRD data indicating that Pd agglomeration has occurred during the experiments, with the wet-VAM catalyst displaying the highest density of particles and strongest Pd-related diffraction peaks.

Table 1. N<sub>2</sub>-physisorption analysis results of calcined-reduced and used catalysts

Description	Units	Calcined-reduced Pd/Al <sub>2</sub> O <sub>3</sub>	Used Pd/Al <sub>2</sub> O <sub>3</sub> , Dry VAM experiment	Used Pd/Al <sub>2</sub> O <sub>3</sub> , Wet-VAM experiment	Used Pd/Al <sub>2</sub> O <sub>3</sub> , Wet-dust-VAM experiment
Langmuir surface area:	m <sup>2</sup> .g <sup>-1</sup>	212.9	167.3	146.5	183.1
Micro-pore area:	m <sup>2</sup> .g <sup>-1</sup>	14.7	21.5	33.2	22.4
BJH adsorption cumulative pore volume	cm <sup>3</sup> .g <sup>-1</sup>	0.7	0.4	0.4	0.5
BJH adsorption average pore diameter	Å	167.6	145.5	158.7	143.7

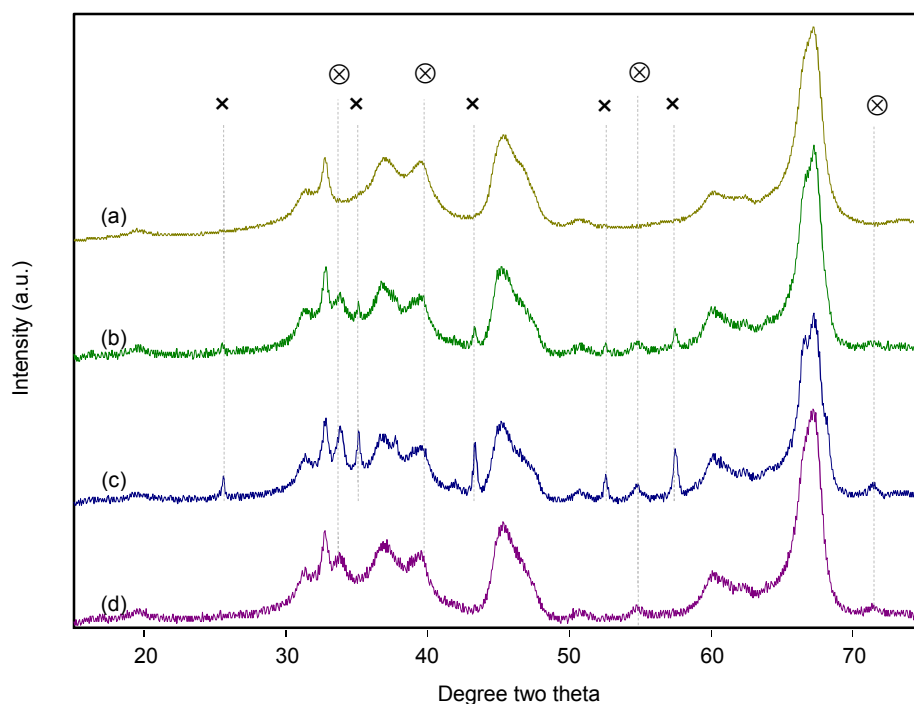


Fig. 2. XRD pattern of (a) calcined-reduced Pd/Al<sub>2</sub>O<sub>3</sub>, (b) used Pd/Al<sub>2</sub>O<sub>3</sub> of dry-VAM experiment, (c) used Pd/Al<sub>2</sub>O<sub>3</sub> wet-VAM experiment, (d) used Pd/Al<sub>2</sub>O<sub>3</sub> of wet-dust VAM experiment. Phase: ⊗ = PdO and × = α-Al<sub>2</sub>O<sub>3</sub>

In order to understand the sintering and re-dispersion process of palladium particles during long-term experiments, the particle size and distribution was assessed using a transmission electron microscope (TEM), shown in Fig. S1 of Supplementary Information (SI). In the calcined-reduced catalyst the palladium particle size ranged from 1 to 5 nm, with the average size of 2.6 nm, explaining why these were difficult to discern in XRD and SEM analyses. On the other hand, in the used samples the average particle size was of the order of 8 nm, indicating that

diffusion and agglomeration of the particles occurred during use.

These data are consistent with a picture in which the initial decay in activity is the result of water adsorption on the support and/or active sites, which are known to occur at low temperatures. This probably accounts for the first stage of deactivation (see Fig. 1), and the presence of water vapour in the feed may simply serve to increase the extent to which this

occurs. Thereafter deactivation continues through loss of active sites via particle agglomeration, and, more slowly, through loss of surface area through phase changes in the support. Both of these occur to a greater extent at higher bed temperatures, although the direct influence of water vapour itself cannot be ruled out. Palladium migration and particle growth occurs in all cases, and is the most prominent when water is present in the feed. Since the final bed temperature was also highest in this case, this could be a simple thermal effect rather than being directly caused by chemisorbed water. However, in the case of the wet feed, XPS suggests that all of the palladium is present as PdO,<sup>8</sup> which presumably also has an impact on activity.

### The activity of aged Pd/Al<sub>2</sub>O<sub>3</sub> catalysts

Light-off curves of total oxidation of methane before and after each catalyst ageing treatment are shown in Fig. 4. In general, these plots suggest that high temperature hydrothermal treatment reduced catalyst activity to levels similar to those seen in the long term tests. The temperature at 90 % methane conversion ( $T_{90}$ ) of the fresh catalyst was 342 °C, whilst for treatment IV it was 412 °C, treatment I was 424 °C, treatment III was 445 °C, and treatment II was 530 °C. Increases in the  $T_{90}$  indicate catalyst deactivation, and these data suggest that

the extent of this is influenced most by treatment temperature, and less by the oxygen partial pressure. These results were used to establish the initial temperatures required for 90 % conversion in TOS testing of the hydrothermal stability of each of the aged catalyst samples.

To observe the deactivation rate, time on stream experiments were performed over the aged catalysts starting at 90 % conversion without increasing the bed temperatures. Fig. 5 illustrates the time on stream behaviours of aged catalysts under treatment I, III and IV. At their respective bed temperatures, the rate of deactivation of the catalyst aged in treatment IV is the lowest. Given the similarity in bed temperatures and light-off curves (Figure 4), this suggests that autoclave aged sample is more stable with respect to deactivation compared to the other two treatments.

The results for treatment III and IV were further examined by adjusting the bed temperature to maintain methane conversion at 90 %, as done in the earlier long-term studies. Fig. 6 indicates that the final bed temperature of treatment III needed to be raised to 500 °C to overcome the deactivation.

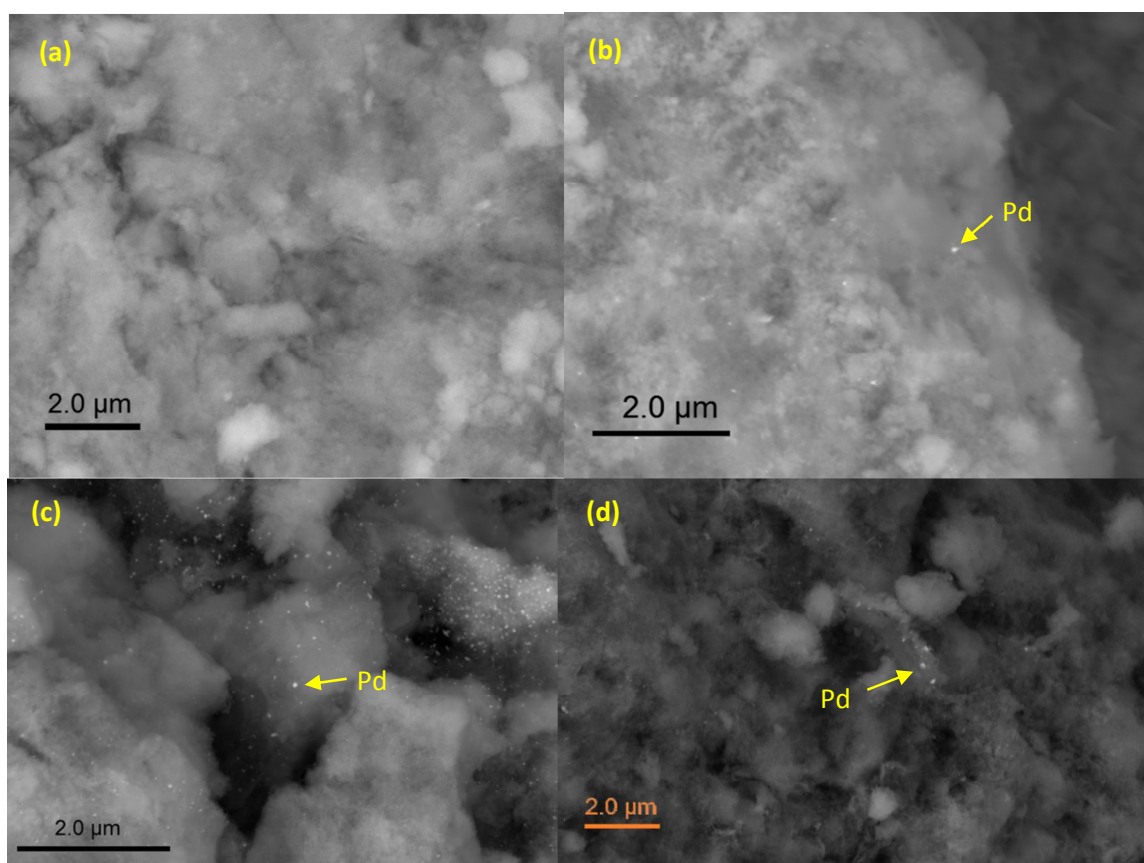


Fig. 3. SEM images of (a) calcined-reduced Pd/Al<sub>2</sub>O<sub>3</sub>; (b) used Pd/Al<sub>2</sub>O<sub>3</sub> from dry-VAM experiment; (c) used Pd/Al<sub>2</sub>O<sub>3</sub> from wet-VAM experiment; (d) used Pd/Al<sub>2</sub>O<sub>3</sub> from wet-dust-VAM experiment

## ARTICLE

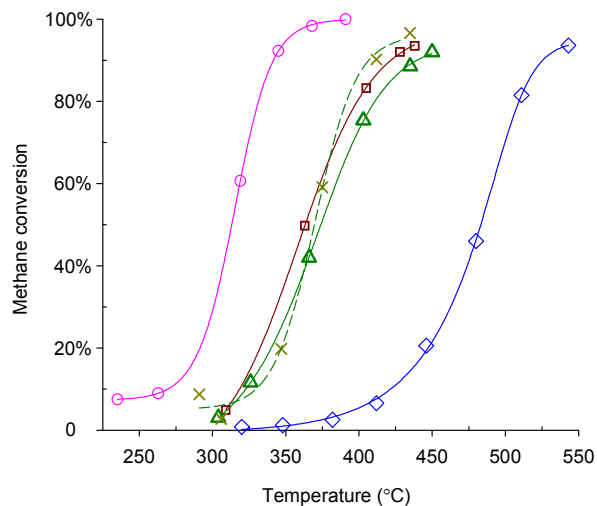


Fig. 4. Methane conversion as a function of temperature over fresh and aged Pd/Al<sub>2</sub>O<sub>3</sub> catalysts. Feed: 0.7 % CH<sub>4</sub>, 3.2 % H<sub>2</sub>O balance air; GHSV = 100 000 h<sup>-1</sup>. ○ = calcined-reduced catalyst; □ = Pd/Al<sub>2</sub>O<sub>3</sub>-I catalysts (aged 18 h in wet feed at 780 °C); ◇ = Pd/Al<sub>2</sub>O<sub>3</sub>-II catalysts (aged 18 h in wet feed at 830 °C); △ = Pd/Al<sub>2</sub>O<sub>3</sub>-III catalysts (aged 18 h in wet O<sub>2</sub> at 780 °C); × = Pd/Al<sub>2</sub>O<sub>3</sub>-IV catalysts (aged 3 days in autoclave at 175 °C).

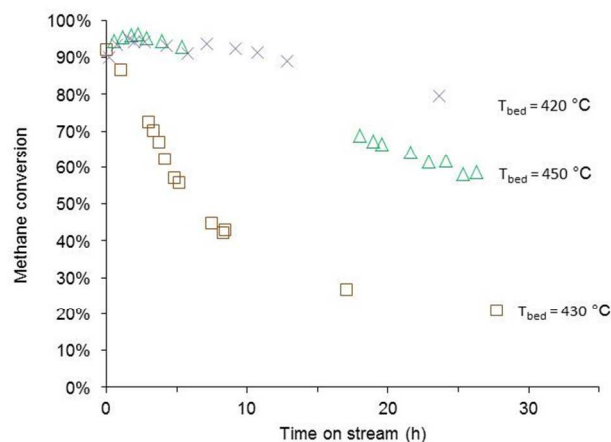


Fig. 5. Time on stream evolution of methane combustion over aged Pd/Al<sub>2</sub>O<sub>3</sub> catalysts. Feed: 0.7 % CH<sub>4</sub>, 3.2 % H<sub>2</sub>O balance air; GHSV = 100 000 h<sup>-1</sup>. □ = Pd/Al<sub>2</sub>O<sub>3</sub>-I catalyst (aged 18 h under wet feed at 780 °C); △ = Pd/Al<sub>2</sub>O<sub>3</sub>-III catalyst (aged 18 h in wet O<sub>2</sub> at 780 °C); × = Pd/Al<sub>2</sub>O<sub>3</sub>-IV catalysts (aged 3 days in autoclave at 175 °C).

This bed temperature is similar to that seen after 1100 h TOS under wet-VAM conditions (see Fig. 1). On the other hand, treating the catalyst in autoclave leads to an increase in stability as the final bed temperature at 28 h TOS remained at 430 °C. However, the catalyst activity continued to decrease over the

first 50 h in methane oxidation tests. The treatments tested, ageing in wet oxidizing mixture at 780 °C for 18 h results in a catalyst behaviour that is the most similar to that of the long-term tests.

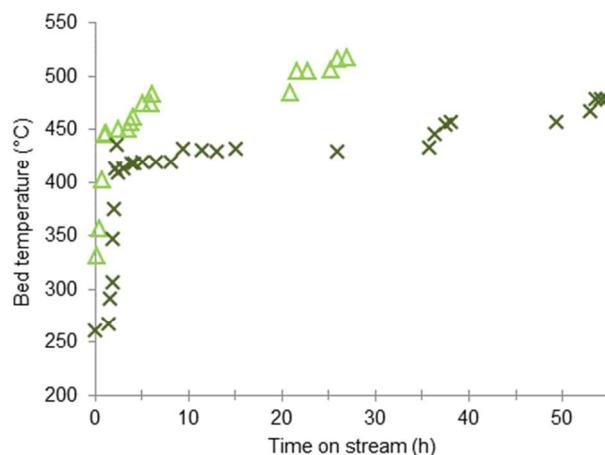


Fig. 6. Catalyst bed temperature required for 90 % CH<sub>4</sub> conversion over △ = Pd/Al<sub>2</sub>O<sub>3</sub>-III catalyst (aged 18 h in wet O<sub>2</sub> at 780 °C) and × = Pd/Al<sub>2</sub>O<sub>3</sub>-IV catalysts (aged 3 days in autoclave at 175 °C). Feed = 0.7 % CH<sub>4</sub>, 3.2 % H<sub>2</sub>O balance air. GHSV = 100 000 h<sup>-1</sup>.

### The nature of aged Pd/Al<sub>2</sub>O<sub>3</sub> catalysts

Nitrogen adsorption-desorption isotherms of the aged catalysts show similarities in comparison to the isotherm of the fresh catalyst. Changes in pore structure and surface area of the aged catalysts are summarised in Table 2. As observed in the long term tests, these results indicate a relatively small change in surface area (of the order of 10 %) with aging in treatment I-III, even at the high bed temperatures used in treatment III. A significant change was found in the catalysts aged in an autoclave where 55 % of the surface area is lost as a result of the treatment. However, the  $T_{90}$  of this catalyst is slightly lower compared to catalysts treatment I and III (see Fig. 4). In this case the significant change in support material pore structures does not result in any major change in active sites. This is supported by TEM results shown in Fig. S4d, where no significant changes were seen in palladium particle size and distribution.

XRD patterns of the aged catalysts are shown in Fig. 7. From treatment I-III catalysts, no changes in the support phases were detected. Analysis of the reflections in the XRD patterns also suggests that no  $\alpha$ -Al<sub>2</sub>O<sub>3</sub> phase was detected in the samples despite the much higher temperatures used compared to the long-term tests, presumably because of the relatively short

treatment times. PdO was only seen in treatment II, although there are some very weak features assigned to this phase in treatment III. The presence of this reflection suggests a growth in the palladium particle size through sintering. Interestingly, the XRD pattern of the treatment IV catalyst as shown in Fig. S2 suggests the formation of AlHO<sub>2</sub> (boehmite) after three days in autoclave at 175 °C. Sharp reflections with high intensity observed in this pattern indicate an increase in crystallinity of the alumina, which is supported by a significant decrease in surface area and the TEM image provided in Fig. S3.

Fig. 8 provides the SEM images of the aged catalysts. Over the surface of the treatment I catalyst, there are a few bright-dots as pointed by arrows in Fig. 8a which were identified as Pd particles by EDS. Upon increasing the ageing temperature to 830 °C (treatment-II), more Pd particles were detected, indicating significant redispersion and crystallite growth. As seen for the long term samples, this crystallite growth is consistent with the appearance of the reflections of a PdO phase seen in the XRD pattern of this sample. Some palladium

particles are also seen on the surface of the treatment-III sample (Fig. 8c).

SEM is limited to detect relatively large particles present on the surface. Fig. S4 provides TEM images of the four aged catalysts including the distribution chart of Pd particle size. TEM particle analysis of the catalyst under treatment I and III (Fig. S4a and S4b) indicates an average palladium particle size of 4 nm after ageing. An increase in particle size was observed in the treatment II sample (Fig. S4b), ranging from 3 to 8 nm. Note that the number of particles observed in the TEM image of the treatment II sample was significantly lower than that seen for the other two aged samples. This is consistent with the XPS data plotted in Fig. 9c where intensities of palladium species detected on the surface are very low compared to other samples, and suggests that Pd depletion occurred under the treatment II conditions. ICP analysis results of the aged samples substantiated the depletion where no decrease in Pd content was observable after the treatments.

Table 2. N<sub>2</sub>-physorption analysis results of aged catalysts

Description	Units	Pd/Al <sub>2</sub> O <sub>3</sub> -I (aged 18 h in wet feed at 780 °C)	Pd/Al <sub>2</sub> O <sub>3</sub> -II (aged 18 h in wet feed at 830 °C)	Pd/Al <sub>2</sub> O <sub>3</sub> -III (aged 18 h in wet O <sub>2</sub> at 780 °C)	Pd/Al <sub>2</sub> O <sub>3</sub> -IV (aged 3 days in autoclave at 175 °C)
Langmuir surface area:	m <sup>2</sup> .g <sup>-1</sup>	193.4	184.5	180.1	96.0
Micro-pore area:	m <sup>2</sup> .g <sup>-1</sup>	2.0	3.8	15.4	13.8
BJH adsorption cumulative pore volume	cm <sup>3</sup> .g <sup>-1</sup>	0.4	0.5	0.5	0.2
BJH adsorption average pore diameter	Å	134.7	147.1	133.1	109.1

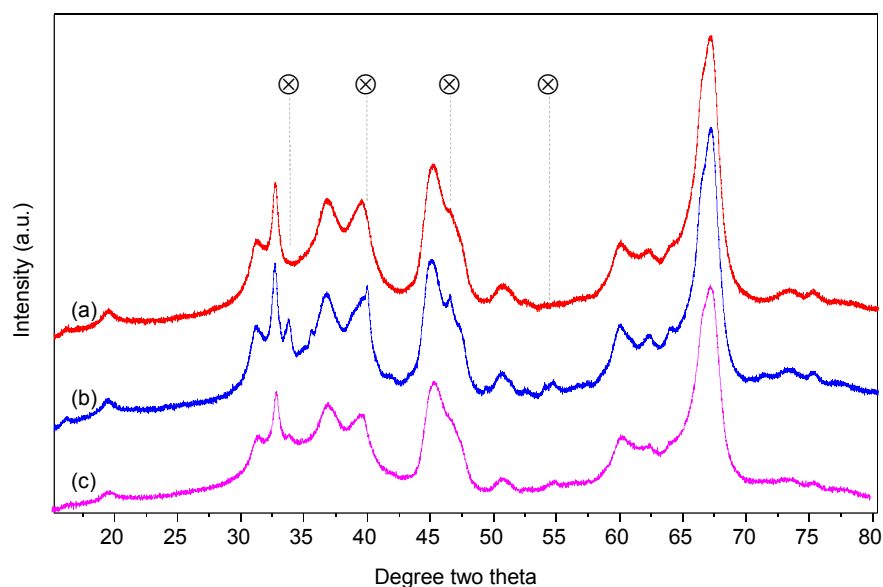


Fig. 7. XRD pattern of aged catalysts (a) Pd/Al<sub>2</sub>O<sub>3</sub>-I catalyst (aged 18 h in wet-feed at 780 °C); (b) Pd/Al<sub>2</sub>O<sub>3</sub>-II catalyst (aged 18 h in wet-feed at 830 °C); (c) Pd/Al<sub>2</sub>O<sub>3</sub>-III catalyst (aged 18 h in wet-O<sub>2</sub> at 780 °C). Phase: ⊗ = PdO.

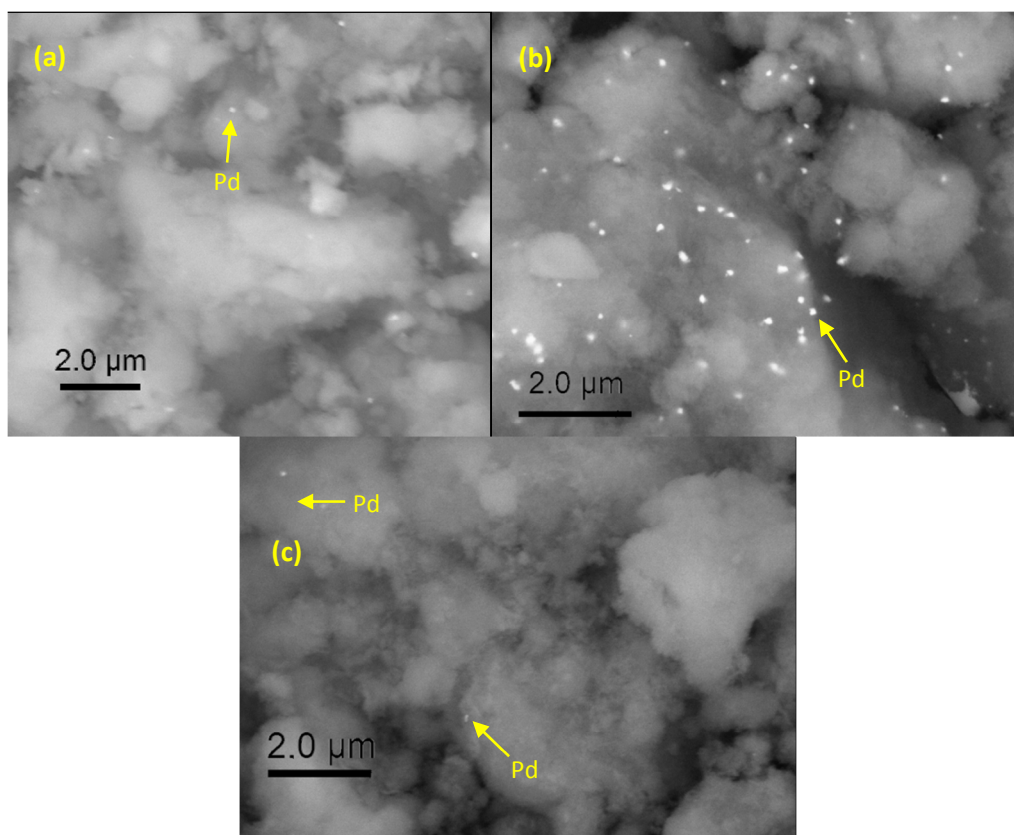


Fig. 8. SEM images of aged catalysts (a) Pd/Al<sub>2</sub>O<sub>3</sub>-I catalyst (aged 18 h in wet-feed at 780 °C); (b) Pd/Al<sub>2</sub>O<sub>3</sub>-II catalyst (aged 18 h in wet-feed at 830 °C); (c) Pd/Al<sub>2</sub>O<sub>3</sub>-III catalyst (aged 18 h in wet-O<sub>2</sub> at 780 °C).

Depletion of Pd is consistent with the significant loss of catalyst activity for this sample that is seen in Figure 4. Both SEM and TEM analyses suggest that palladium migration and particle growth occurs in all cases, although final particle sizes are still smaller than observed in the long term samples.

Fig. 9 represents the XPS spectra of Pd 3d core level of calcined-reduced and aged catalysts. The binding energy (BE) of all fitted peaks and surface compositions are provided in Table 3. XPS analysis results of long-term used catalysts were reported previously.<sup>8</sup> Peak fitting under the spectra of calcined-reduced sample (Fig. 9a) reveals two components detected at Pd 3d<sub>5/2</sub> core-level. These peaks can be identified as Pd<sup>0</sup> (at BE of 335.2 eV) and Pd<sup>2+</sup> (at BE of 336.4 eV).

For treatment I there are also two peaks at BE 334.8 eV and 336.5 eV which are similarly assigned to Pd<sup>0</sup> and Pd<sup>2+</sup> respectively. The intensity of these spectra is lower than that of the fresh catalyst, suggesting a loss of Pd at the catalyst surface during the ageing process. This loss is more extensive in the case of treatment II (see Fig. 9c), and the TEM results suggest that at least some of this loss occurs throughout the sample rather than just at the surface. Treatment II sample also displays peaks assigned to Pd<sup>0</sup> and Pd<sup>2+</sup>, although the PdO:Pd

intensity ratio is the highest of all the samples. The palladium surface depletion is most likely due to diffusion of the Pd into the support to positions deeper than the photoelectron escape depth. This loss is greatest for ageing treatment temperatures close to the decomposition temperature for PdO. This is supported by the XPS data of the long-term used catalysts where no palladium surface depletion was occurred during TOS experiment.<sup>8</sup>

From treatment III catalyst, the XPS spectra after TOS experiment (plotted in Fig. 6) reveal that there is only one Pd species with BEs of 336.8 eV which can be assigned to Pd<sup>2+</sup>. Fitting more peaks under the curve does not give any improvement in fit quality ( $\chi^2$ ). In addition, the Pd surface loss associated with the treatment was similar to treatment I. The oxidation state reached after treatment III is comparable to the oxidation state of catalyst after the long-term wet VAM test where only Pd<sup>2+</sup> was observed in the sample at a concentration of 0.15 at%.<sup>8</sup>

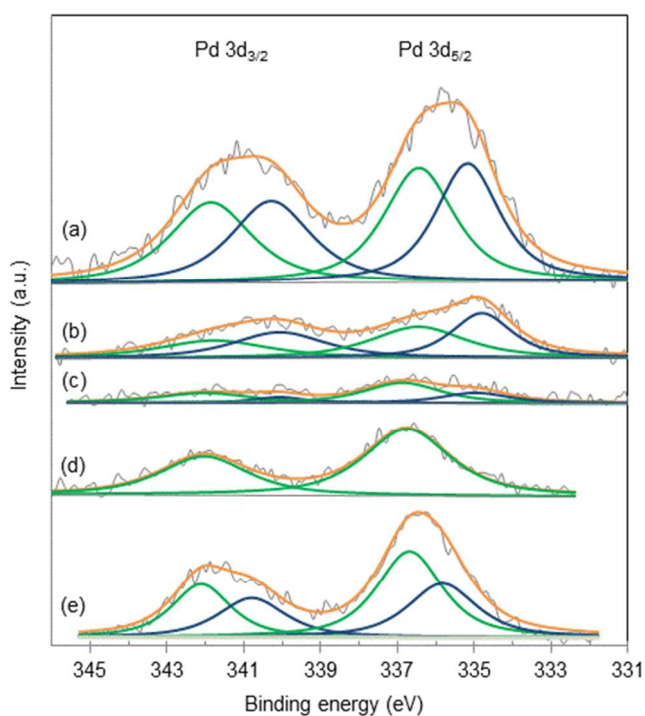


Fig. 9. XPS spectra of Pd 3d core level of 1.0 wt% Pd/Al<sub>2</sub>O<sub>3</sub>, (a) calcined-reduced sample; (b) Pd/Al<sub>2</sub>O<sub>3</sub>-I catalyst (aged 18 h in wet-feed at 780 °C); (c) Pd/Al<sub>2</sub>O<sub>3</sub>-II catalyst (aged 18 h in wet-feed at 830 °C); (d) Pd/Al<sub>2</sub>O<sub>3</sub>-III catalyst (aged 18 h in wet-O<sub>2</sub> at 780 °C); (e) Pd/Al<sub>2</sub>O<sub>3</sub>-IV catalysts (aged 3 days in autoclave at 175 °C).

Table 3. XPS peak position and surface composition

Sample	Pd 3d <sub>5/2</sub> peak position (eV)		Surface composition (%)			
	Pd <sup>0</sup>	Pd <sup>2+</sup>	Pd	O	Al	C
a Pd/Al <sub>2</sub> O <sub>3</sub> , calcined-reduced	335.2	336.4	0.2	59.6	37.7	1.6
b Pd/Al <sub>2</sub> O <sub>3</sub> -I	334.8	336.5	0.1	59.6	38.5	1.8
c Pd/Al <sub>2</sub> O <sub>3</sub> -II	335.0	336.9	0.03	59.9	37.9	2.1
d Pd/Al <sub>2</sub> O <sub>3</sub> -III	-	336.8	0.1	55.1	31.3	10.8
e Pd/Al <sub>2</sub> O <sub>3</sub> -IV	335.8	336.7	0.2	54.8	33.5	9.8

Fig. 9e shows the XPS spectra of treatment IV catalyst after a TOS experiment (plotted in Fig. 6). Similar to the other treatments catalysts, except for treatment III, at Pd 3d<sub>5/2</sub> core level there are two peaks that can be fitted under the curve, Pd<sup>0</sup> at BE of 335.8 eV and Pd<sup>2+</sup> at BE of 336.7 eV. As shown in Table 3, the surface composition of Pd species is similar to the calcined-reduced sample. This information is in-line with TEM analysis results where no significant re-dispersion of palladium particle was found after the treatment.

Activity loss as a result of the hydrothermal ageing appears as a consequence of Pd migration and sintering and possibly

through loss of active species. Once used in a VAM application, these aged catalysts suffer the same rapid decrease in activity thought to be caused by adsorption of water on the support and active sites. None of the ageing tests simulate the change in support phase observed in the long term experiment. These ageing treatments accelerate the deactivation caused by Pd particle sintering. This contributes to activity loss that is likely to be irreversible, particularly if the particles are oxidized. Although oxidized Pd is more active, it is suggested that under humid condition PdO transform into a different structure containing hydroxy groups. This hydroxyl groups accumulate on the catalyst support which can promote re-dispersion process of Pd. XAS measurements are on the way to confirm this behaviour in more detail.

## Conclusions

Insight into catalyst deactivation that occurred during long-term stability tests has been gained by characterizing the used catalysts under N<sub>2</sub>-physisorption, XRD, SEM, TEM and XPS analyses. Deactivation is the result of palladium migration and particle growth and is the most prominent in the presence of water in the feed. The formation of  $\alpha$ -Al<sub>2</sub>O<sub>3</sub> during long-term stability tests explains the changes in pore structures occurred in conjunction with re-dispersion of Pd particles. On the other hand, with a target of mimicking the properties of long-term used catalysts, accelerated ageing of Pd/Al<sub>2</sub>O<sub>3</sub> catalyst was performed under different procedures. XRD patterns of the aged catalysts revealed no  $\alpha$ -alumina phase in the aged catalysts suggesting that the transformation of the alumina phase occurs at a very slow rate. Although it is clear that the aging treatments tested here do not necessarily mimic all of the behaviour observed in the catalyst beds tested on stream over the long-term, ageing under wet-oxygen in helium provides the catalyst bed that is perhaps the closest both in terms of performance and the characterization employed here. The oxidation state reached after treatment III is comparable to the oxidation state of catalyst after the long-term wet VAM test where only Pd<sup>2+</sup> was observed in the sample at a concentration of 0.15 at%. Treating the palladium catalysts at temperatures higher than 780 °C leads to palladium surface depletion which permanently reduces the performance of the catalyst.

## Acknowledgements

Financial support from ACARP is duly acknowledged. A.S thanks the Aceh Province Government, Indonesia for their sponsorship. We thank Jane Hamson for assistance with ICP analysis. We are grateful to the EM/X-ray unit at the University of Newcastle for XRD and SEM analyses.

## Notes and references

<sup>a</sup> Priority Research Centre for Energy (PRCFE), Discipline of Chemical Engineering, School of Engineering, the University of Newcastle, Callaghan, NSW 2308, Australia.

- <sup>b</sup> Mechanical Engineering Department, Faculty of Engineering, Universitas Malikussaleh, Bukit Indah, Lhokseumawe, 24352, Indonesia.
- <sup>c</sup> School of Engineering and Information Technology, Murdoch University, Murdoch, WA 6150, Australia.
- † Footnotes should appear here. These might include comments relevant to but not central to the matter under discussion, limited experimental and spectral data, and crystallographic data.
- Electronic Supplementary Information (ESI) available: [details of any supplementary information available should be included here]. See DOI: 10.1039/b000000x/
- S. Solomon, D. Qin, M. Manning, R. B. Alley, T. Berntsen, N. L. Bindoff, Z. Chen, A. Chidthaisong, J. M. Gregory, G. C. Hegerl, M. Heimann, B. Hewitson, B. J. Hoskins, F. Joos, J. Jouzel, V. Kattsov, U. Lohmann, T. Matsuno, M. Molina, N. Nicholls, J. Overpeck, G. Raga, V. Ramaswamy, J. Ren, M. Rusticucci, R. Somerville, T. F. Stocker, P. Whetton, R. A. Wood and D. Wratt, *Technical Summary*, Cambridge, United Kingdom and New York, NY, USA 2007.
  - H. L. Schultz, P. Carothers, R. Watts and R. McGuckin, *Assessment of the worldwide market potential for oxidising coal mine ventilation air methane*, United States Environmental Protection Agency, Air and Radiation (US-EPA) 2003.
  - P. Gelin and M. Primet, *Appl. Catal., B*, 2002, **39**, 1-37.
  - R. Burch, F. J. Urbano and P. K. Loader, *Appl. Catal., A*, 1995, **123**, 173-184.
  - F. H. Ribeiro, M. Chow and R. A. Dallabetta, *J. Catal.*, 1994, **146**, 537-544.
  - D. Roth, P. Gélin, M. Primet and E. Tena, *Appl. Catal., A*, 2000, **203**, 37-45.
  - D. L. Mowery, M. S. Graboski, T. R. Ohno and R. L. McCormick, *Appl. Catal., B*, 1999, **21**, 157-169.
  - A. Setiawan, J. Friggieri, E. M. Kennedy, B. Z. Dlugogorski and M. Stockenhuber, *Catal. Sci. Technol.*, 2014.
  - W. R. Schwartz, D. Ciuparu and L. D. Pfefferle, *J. Phys. Chem. C*, 2012, **116**, 8587-8593.
  - C. H. Bartholomew, *Appl. Catal., A*, 2001, **212**, 17-60.
  - L. S. Escandon, D. Nino, E. Diaz, S. Ordonez and F. V. Diez, *Catal. Commun.*, 2008, **9**, 2291-2296.
  - S. Specchia, P. Palmisano, E. Finocchio and G. Busca, *Chem. Eng. Sci.*, 2009, **65**, 186-192.
  - M. Honkanen, M. Kärkkäinen, V. Viitanen, H. Jiang, K. Kallinen, M. Huuhtanen, M. Vippola, J. Lahtinen, R. Keiski and T. Lepistö, *Top. Catal.*, 2013, **56**, 576-585.
  - A. Winkler, D. Ferri and M. Aguirre, *Appl. Catal., B*, 2009, **93**, 177-184.
  - Y. Lu, S. Keav, V. Marchionni, G. L. Chiarello, A. Pappacena, M. Di Michiel, M. A. Newton, A. Weidenkaff and D. Ferri, *Catal. Sci. Technol.*, 2014, **4**, 2919-2931.
  - K. S. W. Sing, *IUPAC*, 1982, **54**, 2201-2218.
  - G. D. Carlo, G. Melaet, N. Kruse and L. F. Liotta, *Chem. Commun.*, 2010, **46**, 6317-6319.
  - P. Castellazzi, G. Groppi, P. Forzatti, A. Baylet, P. Marecot and D. Duprez, *Catal. Today*, 2010, **155**, 18-26.
  - H. Arai and M. Machida, *Appl. Catal., A*, 1996, **138**, 161-176.
  - A. K. Neyestanaki, F. Klingstedt, T. Salmi and D. Y. Murzin, *Fuel*, 2004, **83**, 395-408.